

Advanced Digital Signal Processing for High-Capacity Mode-Division Multiplexed Free-Space Optical Communications

[Invited Paper]

Zhouyi Hu¹, Zhaozhong Chen², Yiming Li¹, David M. Benton¹, Abdallah A. I. Ali^{1,3}, Mohammed Patel¹, Martin P.J. Lavery², Andrew D. Ellis^{1,*}

1. Aston Institute of Photonic Technology, Aston University, Birmingham, B4 7ET, UK.

2. James Watt School of Engineering, University of Glasgow, Glasgow, G12 8QQ, UK.

3. Now with Lumensisty Ltd, Unit 7, The Quadrangle, Abbey Park Industrial Estate, Romsey, SO51 9DL, UK.

* E-mail: andrew.ellis@aston.ac.uk

ABSTRACT

Spatial modes provide a potential dimension to boost the capacity of free-space optical (FSO) communication systems. Various modal basis sets can be used. For a given aperture size, complete orthogonal modal basis sets can provide higher capacity compared to incomplete modal basis sets, but are more sensitive to FSO channel impairments, such as atmospheric turbulence. In this invited paper, we review our recent progress in using advanced digital signal processing algorithms for the implementation of high-capacity mode-division multiplexed FSO communication systems when employing complete modal basis sets. Besides turbulence, the relatively high inter-mode crosstalk from a commercial multiplexer/demultiplexer has been taken into account. By employing adaptive loading at the transmitter side and/or advanced multiple-input multiple-output detection algorithms at the receiver side, record-high single-wavelength transmission data rates and spectral efficiency have been achieved over both turbulence-free and turbulent FSO links, where all key devices are commercially available.

Keywords: atmospheric turbulence, digital signal processing, free-space optics, mode-division multiplexing, multiple-input multiple-output, optical wireless communication.

1. INTRODUCTION

Among various modern communication technologies, free-space optical (FSO) communication has attracted much attention, since it is more flexible and more economical than optical fiber communications in some scenarios and offers many advantages such as data rate and security over traditional radio frequency wireless communications [1]. However, there are several negative effects preventing FSO systems from achieving a higher data rate and longer transmission distance, among which atmospheric turbulence is an important one [1].

To overcome the “capacity crunch”, spatial modes provide a potential dimension for space-division multiplexing, i.e., the so-called mode-division multiplexing (MDM), and have been widely studied in FSO systems [2]-[5]. Several modal basis sets have been used for the implementation of MDM-FSO systems, including orbital angular momentum (OAM) modes, Laguerre-Gaussian (LG) modes, Hermite-Gaussian (HG) modes, and linearly polarized (LP) modes. Although OAM is a popular choice [3], it is an incomplete modal basis set, which would provide lower capacity compared to other complete modal bases, e.g., LG, HG and LP modes mentioned above, for a given aperture size [2]. Nevertheless, the complete modes are potentially more sensitive to channel impairments, such as atmospheric turbulence that not only induces intensity fluctuation but also additional inter-mode crosstalk [4].

There are several potential solutions to mitigate atmospheric turbulence effects in MDM-FSO systems. Adaptive optics systems are an efficient scheme that can correct wavefront distortions and partially undo the modal coupling due to atmospheric turbulence [4]. However, such a system would increase the hardware complexity in the optical domain, and cannot fully compensate for the turbulence effects, leading to residual inter-mode crosstalk [4]. Crosstalk mitigation using multiple-input multiple-output (MIMO) digital signal processing (DSP) is an alternative solution that shifts the complexity from the optical to the digital domain [5]. However, the traditional MIMO equalization is only one-stage, which inevitably induces severe noise amplification when the channel transfer matrix is non-unitary (ill-conditioned).

In this paper, we review our recent progress on high-capacity MDM-FSO transmission leveraging advanced DSP algorithms [6]-[9]. We have designed a three-stage MIMO DSP structure that can provide higher flexibility. More powerful MIMO detectors such as interference cancellation (SIC), and maximum likelihood detection (MLD) can therefore be adopted to increase the turbulence resiliency. A generalized MIMO algorithm supporting redundant receive modes has also been demonstrated for more robust transmission. Besides the receiver-side DSP, we have also employed adaptive loading at the transmitter side to maximize the throughput of our system. For MDM implementation, the complete LP modal base was employed, which was excited by a pair of commercial six-mode mode-selective photonic lanterns (MSPLs, Phoenix Photonics, Ltd.) in our system. Despite relatively high inter-mode crosstalk, it demonstrated practical applicability.

2. DSP AND EXPERIMENTAL SETUP

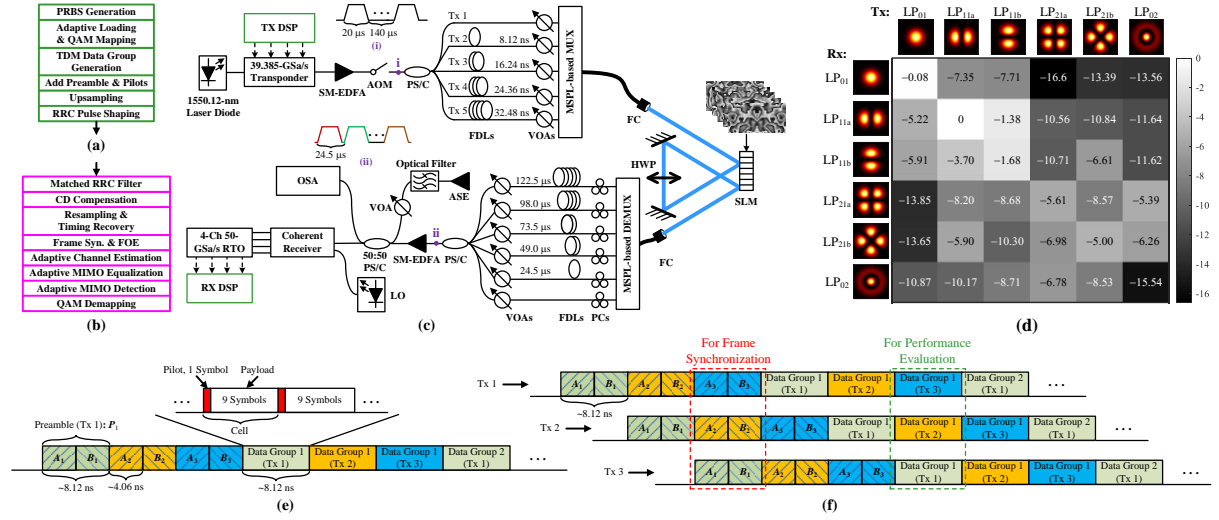


Figure 1. Proof-of-concept experiment for demonstrating a high-capacity MDM-FSO system with turbulence effects: DSP at (a) the transmitter side, and (b) the receiver side, respectively. (c) Experimental setup (ASE, amplified spontaneous emission; EDFA, erbium-doped fiber amplifier; FC, fiber collimator; HWP, half-wave plate; LO, local oscillator; PC, polarization controller; PS/C, power splitter/coupler; VOA, variable optical attenuator); Inset: (i) signal bursts after AOM; (ii) TDM signal bursts after interleaving. (d) Measured crosstalk matrix (dB) of MSPL, normalized to LP_{11a}. Example (e) TDM frames generated at the transmitter side and (f) synchronized streams after power splitter and FDLs (3 transmitters for illustration). [9] © IEEE.

Fig. 1 shows our proof-of-concept experiment for the demonstration of a high-capacity MDM-FSO system with turbulence effects, which is detailed in [9]. The DSP employed at the transmitter side is shown in Fig. 1(a). A pseudorandom binary sequence (PRBS) was first generated for quadrature amplitude modulation (QAM) mapping, where the order of modulation formats (number of bits) and the power were adaptively allocated based on the prior knowledge of channel state information (CSI) [10]. To emulate fully independent transmitters enabling channelized precoding schemes, we used a time-division multiplexed (TDM) frame structure as shown in Fig. 1(e). To demonstrate practical applicability, we used a 39.385-GSa/s commercial transponder (Ciena Wavelic 3) for the generation of a dual-polarization QAM (DP-QAM) optical signal at 1550.12 nm. After amplification, the optical signal was gated by an acousto-optic modulator (AOM) for the implementation of a TDM receiver, where the gate width was 20 μ s with a gate period of 160 μ s as shown in Inset (i) of Fig. 1(c). The burst signals were then split into 5 copies, and delayed by an array of fiber delay lines (FDLs), where the delay time corresponded to the length of data groups of the TDM frame. As shown in Fig. 1(f), the preambles and data groups representing different transmitters were therefore aligned for frame synchronization and performance evaluation respectively. Before launching into the free space, an MSPL was employed for multiplexing. In the FSO channel, we employed a spatial light modulator (SLM) to emulate the turbulence effects [7], [9]. The diameter of the receiver lens (D) was 8.4 mm. The inner scale (l_0) and the outer scale (L_0) of the turbulence were set to 0.1 mm and 10 m, respectively. We can then change the turbulence strength by setting different values of Fried parameter (r_0). A smaller r_0 leads to a stronger turbulence effect.

At the receiver side, the MDM signal was demultiplexed by another MSPL. The measured back-to-back normalized crosstalk matrix of the pair of MSPLs is shown in Fig. 1(d). As we can see, relatively large crosstalk was induced by this pair of commercial devices. The resultant 6 streams, one per mode, were delayed by another array of FDLs with an incremental delay of 24.5 μ s and then combined to produce a TDM stream. These were optically amplified, noise loaded, and detected by a single coherent receiver, this whole process emulating 6 independent receivers. The interleaved signal is illustrated in Inset (ii) of Fig. 1(c). The average optical signal-to-noise ratio (OSNR) of the interleaved signal was measured by an optical spectrum analyzer (OSA). After coherent detection, the resultant electrical signal was captured by a 50-GSa/s four-channel real-time oscilloscope (RTO) for the receiver-side DSP shown in Fig. 1(b). Besides the conventional DSP used in coherent optical systems, we can see from Fig. 1(b) that the proposed three-stage MIMO DSP structure was employed. The channel transfer function matrix was first estimated by the adaptive channel estimator, after which the adaptive MIMO equalization leveraging the estimated channel matrix was applied to the signal before performing MIMO detection. Thanks to this flexible structure, we can employ various MIMO detection algorithms. Four algorithms have been considered: (1) Minimum mean-squared error (MMSE) that is simple but vulnerable to a nonunitary channel; (2) SIC that has better performance than MMSE with a moderate increase in complexity; (3) MLD that is the optimal MIMO detection algorithm but has an extremely high complexity; (4) The proposed combined

SIC-MLD detection algorithm [10] that only applies MLD to the signal vectors that are more likely to be degraded by error propagation after SIC, showing similar performance to MLD-only but much lower complexity.

3. EXPERIMENTAL RESULTS AND DISCUSSIONS

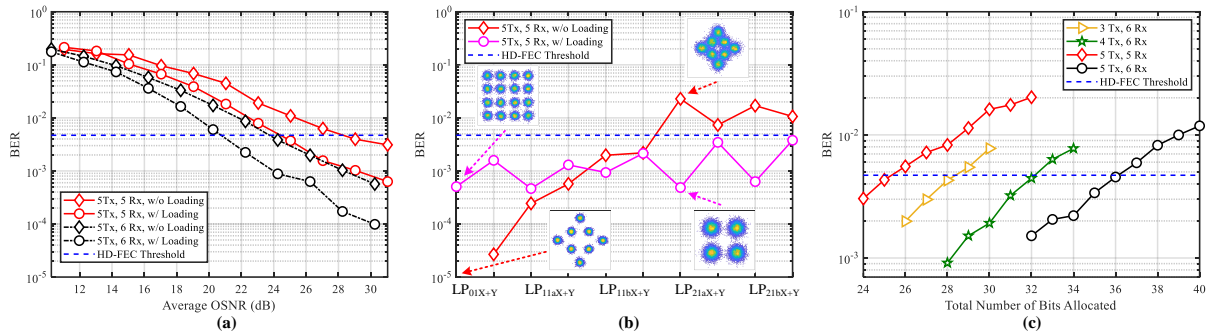


Figure 2. Turbulence-free MDM-FSO transmission: (a) Transmission performance of different signals at the same data rate (30 bits, 29.5 Gbaud). (b) BER versus channel index for the signals with and without adaptive loading (30 bits, 29.5 Gbaud, average OSNR = 27.04 dB). (c) Throughput maximization with adaptive loading and different schemes (36.9 Gbaud). Reprinted with permission from [7] © The Optical Society.

We first demonstrated a record-high net single-wavelength transmission data rate at 1.1 Tbit/s over a turbulence-free multi-modal FSO link using commercial devices, as shown in Fig. 2 [7]. In this work, the SLM-based turbulence emulator was bypassed, but the employed commercial MSPLs still induced relatively large inter-mode crosstalk as depicted in Fig. 1(d). Fig. 2(a) shows the benefits of adaptive loading and redundant receivers on transmission performance in our MDM-FSO system. For a fair comparison, the data rate of all signals was fixed at 885 Gbit/s by allocating 30 bits across all 10 channels (2 polarizations \times 5 modes) and setting the symbol rate to 29.5 Gbaud. We can see from Fig. 2(a) that both adaptive loading and one more receiver can bring on OSNR sensitivity improvement at the hard-decision forward error correction (HD-FEC) threshold of 4.7×10^{-3} . The performance improvement from adaptive loading can be explained by Fig. 2(b). In the case without adaptive loading, the bit-error rate (BER) of different channels shows a very large fluctuation due to the difference in SNR in our MIMO system. Meanwhile, this problem can be effectively solved by allocating different modulation formats and power to different channels based on the CSI estimated before transmission [10]. The average BER is thus reduced from 6.28×10^{-3} to 1.56×10^{-3} , meeting the requirement of HD-FEC. We have then maximized the throughput of our turbulence-free MDM-FSO system by leveraging adaptive loading, as shown in Fig. 2(c). Herein, we varied the number of transmitters and the total number of bits allocated. The number of receivers was fixed at six, except the case with five transmitters and five receivers was attached as the benchmark. The symbol rate was set to 36.9 Gbaud for all cases. We can see from the figure that by enabling the first five modes for carrying data, we successfully achieved a maximum line rate of ~ 1.33 Tbit/s (36 bits \times 36.9 Gbaud). After considering all overhead, the net data rate and the net spectral efficiency achieved in this work were ~ 1.1 Tbit/s/wavelength and 28.35 bit/s/Hz, respectively, which were both record-high when all key devices were commercially available for turbulence-free MDM-FSO transmission.

As shown in Fig. 3, we have also verified the feasibility of the advanced DSP for the enhancement of turbulence resiliency in MDM-FSO systems by enabling the SLM-based turbulence emulator. In Fig. 3(a) and Fig. 3(b) [8], the symbol rate was set to 34.46 Gbaud, uniform DP-4-QAM symbols were used, and r_0 was set to 0.8 mm ($D/r_0 = 10.5$). In Fig. 3(c) [9], the symbol rate was set to 29.5 Gbaud, uniform DP-4-QAM symbols were used when adaptive loading was disabled, and r_0 was set to 0.5 mm ($D/r_0 = 16.8$). In both Fig. 3(a) and Fig. 3(c), the number of transmit modes (N_t) and receive modes (N_r) was set to 5 and 6, respectively, leading to a line rate of 689.23 Gbit/s and 590 Gbit/s, respectively. We can see from Fig. 3(a) that under 120 weaker turbulence realizations ($D/r_0 = 10.5$), the BER of the SIC system is consistently lower than the MMSE system. As a result, the average BER among different turbulence realizations is decreased by an order of magnitude from 8.02×10^{-3} in the MMSE system to 4.76×10^{-4} in the SIC system. In Fig. 3(b), we also compared the transmission performance of different transmit and receive mode numbers in turbulence, where the average BER is calculated using the same 120 independent patterns. The results indicate that both SIC and increasing the number of receive modes can enhance atmospheric turbulence resiliency. We finally combined the transmitter-side and the receiver-side DSP, and verified the performance of the whole system under 12 stronger turbulence realizations ($D/r_0 = 16.8$). The results show that combining adaptive loading and more powerful MIMO decoders can bring on the reduction of BER not only compared to the conventional scheme without adaptive loading and with simple MMSE detection, but also the scheme only with adaptive loading or only with powerful MIMO decoders. The combined SIC-MLD (10% MLD) has a similar curve and only shows a marginal degradation compared to MLD-only, indicating its similar performance but much lower computational complexity.

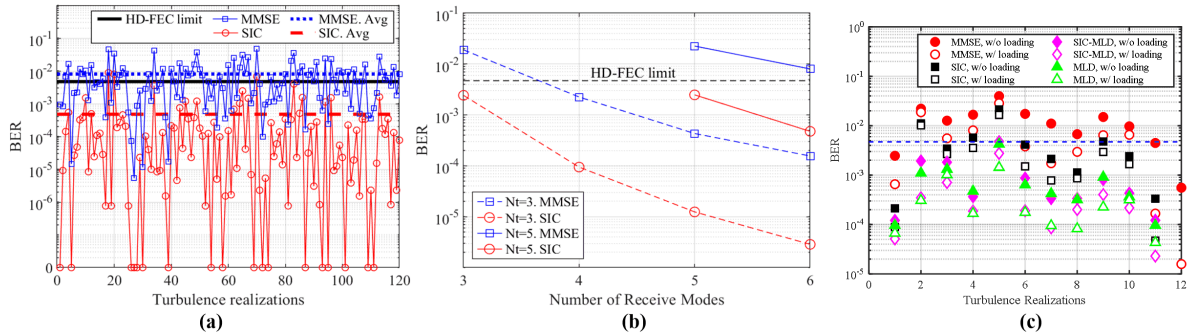


Figure 3. MDM-FSO transmission in turbulence: (a) The BER performance of the MDM-FSO system ($N_t = 5$, $N_r = 6$) with different MIMO decoders (without adaptive loading) under 120 weaker turbulence realizations ($D/r_0=10.5$) [8] © IEEE. (b) The average BER performance of different MIMO systems (without adaptive loading) under 120 weaker turbulence realizations ($D/r_0=10.5$) [8] © IEEE. (c) The BER performance of the MDM systems ($N_t = 5$, $N_r = 6$) with different transmitter-side and receiver-side DSP schemes under 12 stronger turbulence realizations ($D/r_0=16.8$) [9] © IEEE.

4. CONCLUSIONS

In this invited paper, we have reviewed our recent progress in using advanced DSP for the implementation of high-capacity MDM-FSO systems. A proof-of-concept experiment has been introduced, which can emulate multiple independent transmitters and receivers, enabling channelized DSP at both the transmitter and the receiver sides. An SLM-based turbulence emulator can impose variable turbulence effects on the FSO beam. With the help of advanced DSP algorithms, we have demonstrated a record-high 1.1-Tbit/s net single-wavelength transmission data rate over a turbulence-free multi-modal FSO link, and a line rate of 689.23 Gbit/s and 590 Gbit/s when weaker ($D/r_0=10.5$) and stronger ($D/r_0=16.8$) turbulence effects were applied, respectively.

ACKNOWLEDGEMENTS

This work was partly supported by EPSRC under grant numbers EP/T009047/1, EP/T009012/1, EP/S003436/1, and EP/S016171/1; European Union’s Horizon 2020 research and innovation programme under the Marie Skłodowska-Curie grant agreement No. 713694; Future and Emerging Technologies Open grant agreement Super-pixels No. 829116.

We would like to thank Ciena and Dr. Charles Laperle for kindly providing the WaveLogic 3 transponder used in our experiments.

REFERENCES

- [1] A. Trichili *et al.*, “Roadmap to free space optics,” *J. Opt. Soc. Amer. B*, vol. 37, no. 11, pp. 184–201, 2020.
- [2] N. Zhao, X. Li, G. Li, and J. M. Kahn, “Capacity limits of spatially multiplexed free-space communication,” *Nat. Photon.*, Vol. 9, no. 12, pp. 822–826, 2015.
- [3] A. E. Willner *et al.*, “Perspectives on Advances in High-Capacity, Free-Space Communications Using Multiplexing of Orbital-Angular-Momentum Beams,” *APL Photonics*, vol. 6, no. 3, 2021, p. 030901.
- [4] Y. Ren *et al.*, “Adaptive-optics-based simultaneous pre-and post-turbulence compensation of multiple orbital-angular momentum beams in a bidirectional free-space optical link,” *Optica*, vol. 1, no. 6, pp. 376–382, 2014.
- [5] H. Huang *et al.*, “Crosstalk mitigation in a free-space orbital angular momentum multiplexed communication link using 4×4 MIMO equalization,” *Opt. Lett.*, vol. 39, no. 15, pp. 4360–4363, 2014.
- [6] Y. Li *et al.*, “Demonstration of 10-channel mode-and polarization-division multiplexed free-space optical transmission with successive interference cancellation DSP,” *Opt. Lett.*, vol. 47, no. 11, pp. 2742–2745, 2022.
- [7] Z. Hu *et al.*, “Single-wavelength transmission at 1.1-Tbit/s net data rate over a multimodal free-space optical link using commercial devices,” *Opt. Lett.*, vol. 47, no. 14, pp. 3495–3498, 2022.
- [8] Y. Li *et al.*, “Enhanced Atmospheric Turbulence Resiliency with Successive Interference Cancellation DSP in Mode Division Multiplexing Free-Space Optical Links,” *J. Lightw. Technol.*, Vol. 40, no. 24, pp. 7769–7778, 2022.
- [9] Z. Hu *et al.*, “Adaptive Transceiver Design for High capacity Multi modal Free-space Optical Communications with Commercial Devices and Atmospheric Turbulence,” *J. Lightw. Technol.*, 2023 (early access, DOI: 10.1109/JLT.2023.3242215).
- [10] P. S. Chow *et al.*, “A practical discrete multitone transceiver loading algorithm for data transmission over spectrally shaped channels,” *IEEE Trans. Commun.*, vol. 48, pp. 772–775, 1995.